A Low-Cost Ground Truth Marker System for Localization Algorithm Evaluation

Ahmet Kağızman[1]*, Ozan Vahit Altınpınar[1] and Volkan Sezer[2]

[1] Istanbul Technical University, Institute of Science, Smart and Autonomous Systems Laboratory, SASLab, Ayazaga Campus, 34469 Maslak/Istanbul/Turkey, kagizman@itu.edu.tr; altinpinaro@itu.edu.tr

[2] Istanbul Technical University, Department of Control and Automation Engineering, Smart and Autonomous Systems Laboratory, SASLab, Ayazaga Campus, 34469 Maslak/Istanbul/Turkey, sezerv@itu.edu.tr

* Corresponding author

Abstract: Localization is one of the most critical technical problems of autonomous robots. To evaluate the performance of any localization algorithm, the ground truth data is required for comparison. On the other hand, high-cost, complex, and limited-area effective, precise camera systems are utilized to obtain accurate position information. In this study, a novel device has been developed and produced as an alternative to existing systems. It is simple, low-cost, easily integrated into many robots, and capable of leaving a mark directly on the ground, making it effective throughout the robot's motion regions. During the testing process, the position of each mark was measured manually to confirm the accuracy of the measurements taken by the device, which was mounted on the autonomous wheelchair and automatically left marks on the ground, at certain numbers and intervals. The data obtained with the device have been compared with Adaptive Monte Carlo Localization (AMCL), a localization algorithm, and Odometry data. As a result of this comparison, it has been observed that the Odometry-based prediction vector initially closely matched the ground truth data but accumulated errors over time. In the AMCL algorithm, however, although instant position errors may occur using Lidar measurement data taken from the surroundings, these errors have been determined to decrease significantly in the next steps. As a result, it has been confirmed that the obtained results are compatible with theoretical expectations.

Keywords: Localization; ground truth; AMCL; odometry; autonomous robots

1 Introduction

Currently, autonomous robots can successfully perform various and comprehensive tasks in many fields, from industrial production processes [1] to agriculture [2] [3], from education [4] to the transportation sector [5], and from healthcare [6] to

academic research [7] [9]. This versatile use of autonomous robots has become increasingly becoming widespread to optimize business processes, increase efficiency, and support manpower. These robots need environmental information to move safely and accurately. This environmental information is a basic need for the robot to perform actions such as moving from one position to another or picking up an object from one place and taking it to another place. However, to perform these tasks, the robot must accurately determine its position and orientation in its environment. This situation, known as localization, is one of the most fundamental problems of autonomous robots [10-13].

In general, the pose components of ground robots are the position of the robot in x-y coordinates (x_r, y_r) and the orientation of the robot (θ_r). The localization process is performed by utilizing sensor data on the map where the robot is located and taking into account past position information. In this stage, the robot perceives specific features in its surroundings and updates its position using various probabilistic approaches based on these perceptual results. However, determining the accuracy of the prediction at this point is a critical step in evaluating the effectiveness of localization. To analyze how accurately the robot makes this prediction, it is necessary to obtain ground truth information about where and in what orientation it is on the map [14-16]. The developed localization algorithms' performance and prediction accuracy can only be evaluated by comparing them with this ground truth information. In autonomous robot systems, obtaining ground truth information is achieved by taking simultaneous images from multiple cameras, as depicted in Figure 1, and processing these images [17-21].

Figure 1

Traditional motion capture systems which is used to obtain ground truth data in autonomous robots

However, these sensitive cameras that must be used and the computer system in which the data obtained from these cameras will be processed both complicate the

system itself and its installation and present an extremely costly solution [20-23]. Furthermore, since existing systems providing position information are set up to cover a limited area, the visibility of the robot on the ground by the cameras may not always be feasible [22] [23]. For this reason, the working environment needs to be conducive to placing cameras at an optimal height. Such height restrictions and focusing on a specific area prevent autonomous robots from working effectively in a wide environment [24].

In this study, a novel low-cost device that adopts a simple design and can be easily mounted on many robots was developed and fabricated as an alternative to complex, high-cost, and multi-unit systems to obtain ground truth position and orientation information of autonomous ground robots [25]. This developed device enables obtaining ground truth information in desired regions through the marks it directly leaves on the ground, thereby providing the opportunity to analyze how erroneous the pose information calculated by the robot is. In addition, thanks to this feature, it is not only effective in a certain area, as in traditional camera-based solutions, but also provides a wide usage area along the trajectory of the robot on which it is integrated. The effectiveness of this device, manufactured with today's production facilities, has been tested through Adaptive Monte Carlo Localization (AMCL), a localization algorithm, and the Odometry method, which calculates the location using only the information from the encoders of the mobile robot [26] [29]. In this testing process, our self-developed autonomous wheelchair has been used as the ground robot model.

Although previous studies have presented various methods for evaluating the localization performance of autonomous ground robots, most rely on expensive and complex motion capture systems. In contrast, this study introduces a low-cost ground truth marker system whose total cost is less than 1% of traditional multi-camera systems. This system offers a practical and easily deployable solution that enables pose evaluation throughout the robot's entire operational environment. In addition, an original mechatronic design and a customizable control interface are proposed. To the best of our knowledge, this is the first study to describe such a system in detail and validate its performance in a real-world localization scenario using AMCL and odometry within the Robot Operating System (ROS) framework.

The remainder of this article proceeds as follows: Section 2 consists of the mechanical design and fabrication of the developed device, while Section 3 comprises electronic design and software components. The tests performed and their results are presented in Section 4. Finally, the conclusions and future research studies are described in Section 5.

2 Mechanical Design and Fabrication of the Developed Device

This section presents a comprehensive overview of the mechanical design and fabrication processes undertaken in the development of the ground truth marker device.

2.1 Mechanical Structure of the Ground Truth Marker Device

The developed ground truth marker device features a compact mechanical structure comprising a servo-driven rack-and-pinion mechanism mounted on a modular chassis, which allows easy integration into various autonomous ground vehicles. The pinion gear, attached to the motor shaft, engages with the rack to convert rotational motion into vertical motion, enabling up and down movement. Mounted on the rack, a telescopic vertical arm enables height adjustment to accommodate autonomous ground robots of different sizes. Additionally, a drill-chuck-like diameter adjustment mechanism allows manual tightening or loosening of markers with varying diameters. To ensure smooth and stable ground markings without harshly touching the ground, a spring is placed between the chuck body and the telescopic structure. The mechanical design of the system is illustrated in Figure 2.

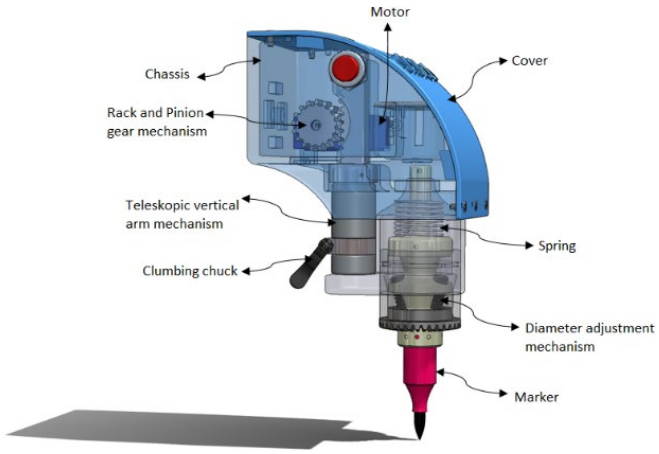

Figure 2
Mechanical design of the developed ground truth device

2.2 Fabrication and Integration of the Mechanical Components

The mechanical components of the developed device were fabricated via 3D printing using selected thermoplastic materials. Tough PLA (Porima, Türkiye) was employed for the chassis, cover, telescopic vertical arm structure, and the diameter

adjustment mechanism due to its structural stability and dimensional consistency. For the rack and pinion gear set, which requires high mechanical performance, PC/ABS FR (Ultrafuse, BASF, Germany) was preferred for its superior wear, impact, and heat resistance, ensuring reliable torque transmission [30]. In components such as the clamping chuck, Nylon (Ultimaker, Netherlands) material was specifically used to provide the required flexibility for locking functionality. In addition to these components, various integration apparatuses – including angled, suction cup, and bolted types – were developed to enable the mounting of the device onto autonomous ground vehicles via the chassis. While angled apparatuses allow adaptation to inclined surfaces, suction cup modules ensure firm adhesion to flat surfaces and minimize vibration. The bolted apparatuses, in contrast, are used for rigid and more permanent installations. These integration components were also fabricated using Tough PLA, ensuring material consistency across the system. Following the fabrication of these mechanical and integration components, the assembly process was carefully planned and executed. Figure 3 (a) presents the fully assembled device. Figures 3 (b) and 3 (c) illustrate its integration onto an autonomous wheelchair and the Turtlebot 3 platform [31], which was developed by Open Robotics, using bolted apparatuses. Figure 3 (d) demonstrates the mounting of the device onto the autonomous wheelchair using both angled and suction cup apparatuses simultaneously.

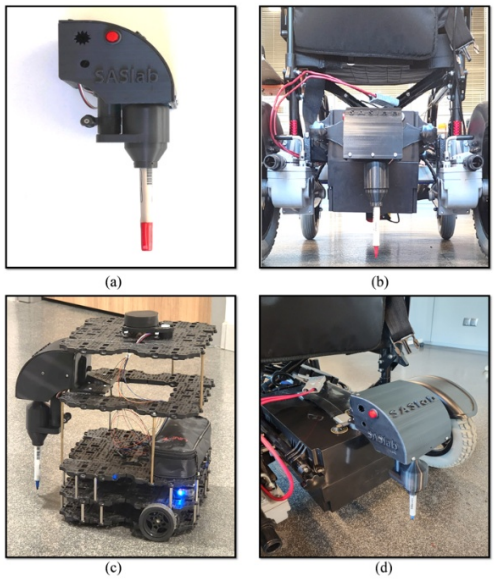

Figure 3

The developed ground truth marker device (a); integration of the device onto an autonomous wheelchair (b) and the Turtlebot 3 platform (c) using bolted apparatuses; and installation onto the autonomous wheelchair using both suction cup and angled apparatuses (d)

3 Electronic Architecture and Software Framework of the Developed System

This section presents the electronic architecture and embedded software components developed for the ground truth marker device. It covers the hardware design and integration of the electronic control unit, the implementation of a user interface for system monitoring and interaction, and the communication infrastructure that enables seamless integration with the ROS platform.

3.1 Design and Implementation of the Electronic Control System

To enable electronic control and system integration, a custom-designed PCB (Printed Circuit Board) was developed following the mechanical fabrication of the device. Designed using the EAGLE platform and fabricated through standard PCB etching, the board facilitates servo motor control and wireless transmission of orientation data from the onboard IMU (Inertial Measurement Unit) to a main computer. It integrates several key components, including an Arduino Nano microcontroller, a BNO055 IMU, an HC-05 Bluetooth module, an NRF24L01 transceiver, and an MP1584EN step-down voltage regulator, each performing specific functions within the system.

The Arduino Nano is utilized in both the transmitter and receiver units to handle peripheral sensor communication and data processing. Among these peripherals, the BNO055 IMU, connected to the microcontroller via the I²C protocol, provides real-time orientation and motion data. The HC-05 Bluetooth module enables servo motor control and timing adjustment of the marker's contact with the ground. The NRF24L01 transceiver module enables low-power wireless communication between the transmitter and receiver units [32]. This sensor transmits the orientation data obtained from the BNO055 IMU and the time at which the marker touches the ground to the receiver unit, which then relays this information to the main computer via Arduino Nano. The orientation information in the ground truth data can be obtained by manually measuring the orientation angle of the mark left on the ground or directly by using the information provided by the IMU on the device. This IMU sensor provides high-precision yaw, pitch, and roll measurements in the three-dimensional Euclidean space R^3, processing raw data from its onboard accelerometer, gyroscope, and magnetometer via a 32-bit ARM Cortex-M0+ processor in fusion mode with advanced filtering to yield accurate and reliable orientation estimates.

Finally, The MP1584EN voltage regulator is employed to convert the 11.1 V battery output to a suitable level for the servo motor. Figure 4 illustrates the placement of the PCB, battery, and motor on the device chassis.

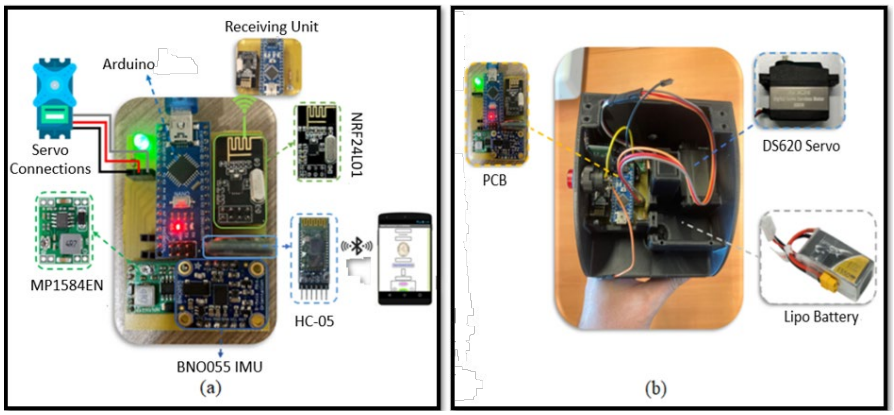

Figure 4
(a) Integrated electronic components on the custom PCB
(b) Placement of the PCB, battery, and servo motor on the device chassis

3.2 Interface Design and ROS-Based Communication

The device is remotely controlled via an Android-based interface developed with MIT App Inventor, with communication provided through the HC-05 Bluetooth module [33]. The interface offers two operation modes for ground marking: automatic (with a predefined period T) and manual. After establishing a Bluetooth connection (Figure 9 (a)), users can access the motor control panel (Figure 9 (b)), where commands such as START, STOP, and RESET manage the servo operation. The system allows fine-tuning of ground contact duration in 100-ms increments and provides quick access buttons to adjust airtime. Manual marking can be initiated at any time by pressing the "MAN" button. This interface is shown in Figure 5.

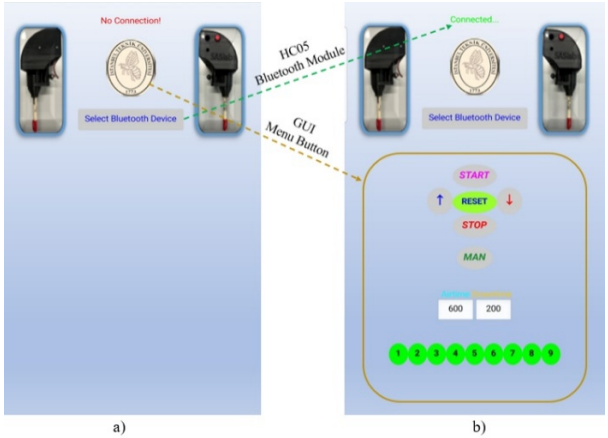

Figure 5
The first view of the interface (a), view after pressing the GUI menu button (b)

When operating in automatic mode, the periodic change in the marker's height relative to the ground over time is illustrated in Figure 6. At time t_1, a PWM signal is sent to the servo motor by the microcontroller and the marker is caused to descend on the ground. The descend time is $t_2 - t_1$, after which the marker remains in tounch with the ground to leave a visible mark for a time of $t_3 - t_2$, depending on the speed of the mobile robot. At time t_3, another PWM signal triggers the marker to return to its previous position, completing this movement at t_4. After the marker remains in the air for about $t_5 - t_4$ seconds, a PWM signal is sent to the marker again at time t_5 and this process continues periodically. The total time the marker stays in the air (Airtime) and on the ground (Downtime) is mathematically expressed as $(t_2 - t_1) + (t_5 - t_3)$ and $(t_3 - t_2)$ seconds, respectively. The maximum height h of the marker from the ground has been adjusted to be approximately 2 cm. In manual mode, the airtime of the marker depends on how long the "MAN" button is pressed, resulting in non-periodic motion. As shown in Figure 7, the device operates based on the selected mode – manual or automatic. While automatic mode enables comprehensive performance evaluation across the entire map, manual mode allows focused measurements in a specific region to assess local pose estimation performance.

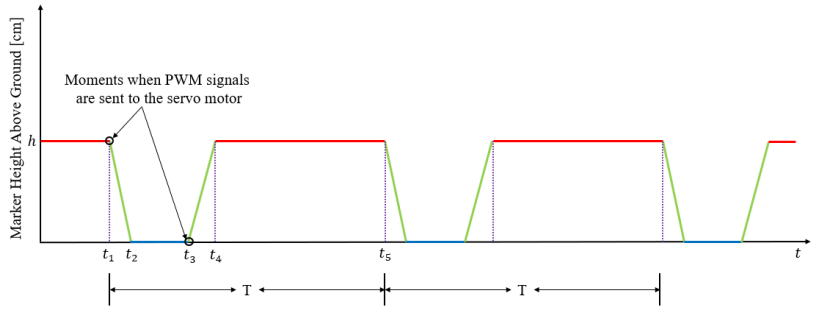

Figure 6

Variations of marker's height from the ground, over time, during device operation in automatic mode

In both operation modes, the mark on the ground and the orientation angle information are transmitted to the main computer via the receiver unit. This communication is handled in the ROS environment, where the transmitted data is published as topics [34]. Thus, all pose-related data can be systematically logged, synchronized, and utilized in real time by the localization algorithm.

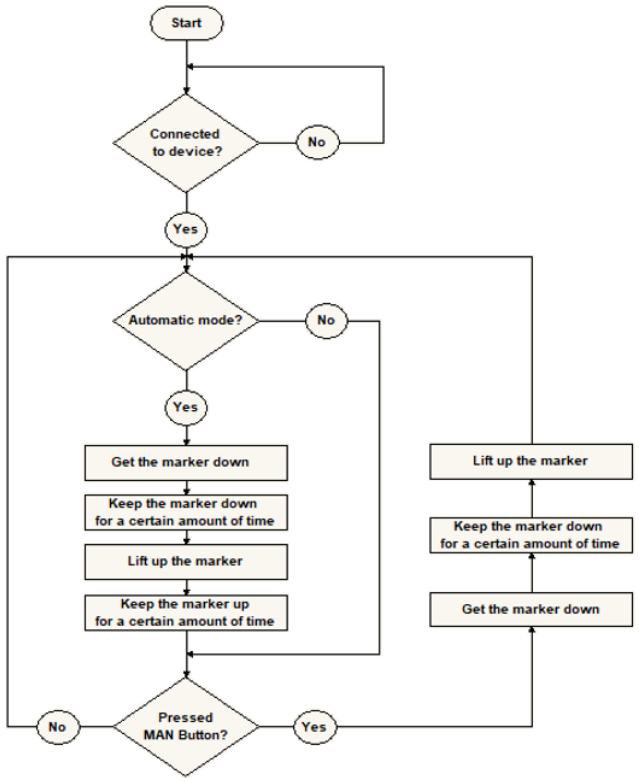

Figure 7
The flowchart of the device's operating algorithm

4 Tests and Results

In this section of the study, firstly, the experimental platform in which the developed device is used and the environment in which the experiments are carried out has been explained in detail. Additionally, information has been provided on how ground truth data is obtained. Finally, to test the device's performance, the results obtained with the device are compared with AMCL and Odometry methods.

4.1 Experimental Platform and Data Collection Environment

To evaluate the performance of the proposed device in a real-world environment, a custom-built autonomous wheelchair was utilized as the experimental platform. Equipped with multiple onboard sensors, including a Lidar, RGB-D camera, IMU, and wheel encoders, this robotic system operates under the ROS platform and

supports both autonomous and semi-autonomous control modes [14]. The physical integration of the developed marker device with the wheelchair as seen in Fig. 8.

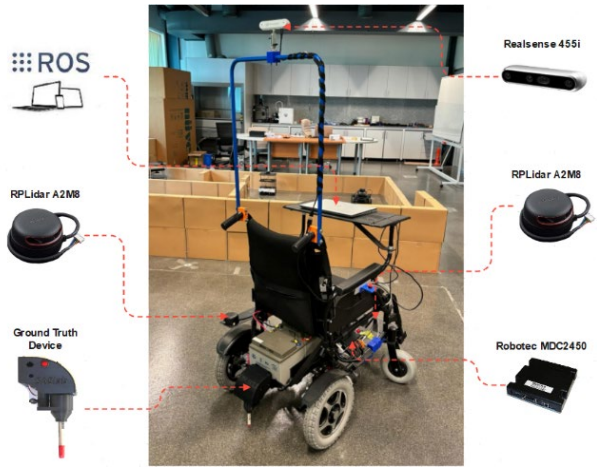

Figure 8

Hardware configuration of the experimental platform used for validation

The experimental environment was established in the corridor of the Smart and Autonomous Systems Laboratory, located within the Faculty of Electrical and Electronics Engineering at Istanbul Technical University. An occupancy grid map of this corridor was generated using the Gmapping package of the ROS platform. This map plays a critical role in enabling the mobile robot to perceive its environment and accurately estimate its position within the test area. The layout of the experimental corridor and the corresponding occupancy map are illustrated in Figure 9.

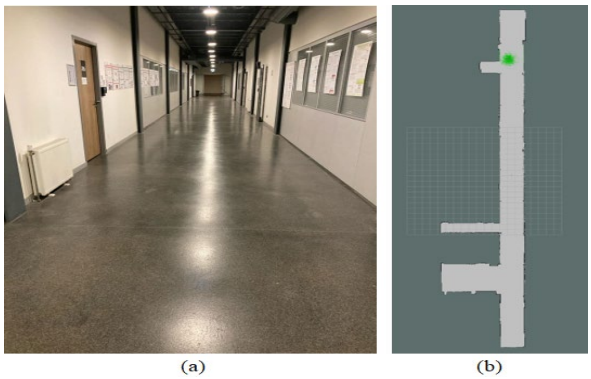

Figure 9

Experimental corridor (a) and its corresponding occupancy map (b)

To manually measure the ground truth data on this corridor, two reference points spaced five meters apart were determined. Each mark left on the ground was measured relative to its nearest reference point, a method adopted to facilitate manual measurements and improve the accuracy of the collected data. The starting point of the trajectory was set as the center of the first reference point, and the device was positioned so that the tip of its marker aligned precisely with this center. The autonomous wheelchair's speed was set to 0.25 m/s on straight paths, with the device operating at a period of approximately 1.7 seconds. During turning maneuvers, the speed was automatically reduced to a value close to zero to ensure precise and safe operation. Subsequently, as the system moved, the device was operated in automatic mode along its trajectory, leaving 23 physical marks on the ground over a total distance of 8.05 meters. The position of each mark was manually measured and recorded by two individuals using a measuring tape and a caliper, according to the determined reference points. To verify accuracy and identify potential errors, these measurements – completed in approximately 58 minutes – were compared against readings from a laser measuring device (UNI-T LM50A, millimeter-level precision), revealing a deviation of 2.94 cm over the 8.05-meter distance. Although the autonomous wheelchair covered this distance in just 37 seconds, the manual collection of position data required considerable physical effort due to the repetitive bending and precise alignment involved. The determined reference points, the marks left on the ground, and the manual measurements made are shown in Figure 10. The video showing the basic accuracy test performed with the autonomous wheelchair can be accessed from the link below. https://drive.google.com/file/d/1VQ4EjsZzmiLke9iXhUzIEv3JK6EPTYiI/view?usp=sharing

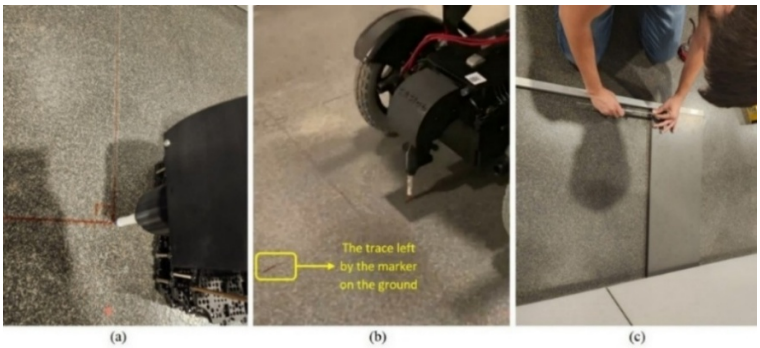

Figure 10
Reference points (a), mark left on the ground (b) and manual measurements (c)

4.2 Localization Test Results

Localization, the problem of mobile robots estimating their position, is one of the most critical research areas in the field of autonomy [35]. The positions of these robots can be calculated through the information obtained from their motion

kinematics and the encoders mounted on their wheels. However, in real-world applications, errors that cannot be underestimated may occur due to factors such as encoder measurement error, noise, displacement of the robot while moving, or sudden slippage. Additionally, in wheelchairs with caster wheels, sudden rotation of these wheels can cause serious position errors. Due to the mentioned factors, position errors calculated with encoder data cannot be corrected and increase cumulatively over time. Although there are many algorithms introduced in the literature to minimize these errors, Kalman and Particle filter-based algorithms are the most popular [10] [36]. To test the accuracy of localization algorithms, on the other hand, ground truth information is needed. To test the effectiveness of the developed device, the ground truth data obtained using the device has been compared with the AMCL algorithm and the Odometry method, which calculates the position using only the information from the encoders of the mobile robot. To make this comparison, the marks left by the developed device on the ground must first be transferred to the base link of the URDF (Universal Robot Description Format) model on the ROS platform of the mobile robot [7]. Because the position estimates of the algorithms running on the ROS platform are compared with the current position of the base link of the mobile robot's URDF model. The origin of the base link is usually the geometric center of the mobile robot. According to the trajectory shown in Figure 11, the position of the mark left on the ground can be transformed into the mobile robot's base link frame using the known distance l between the marker and the robot's base link origin.

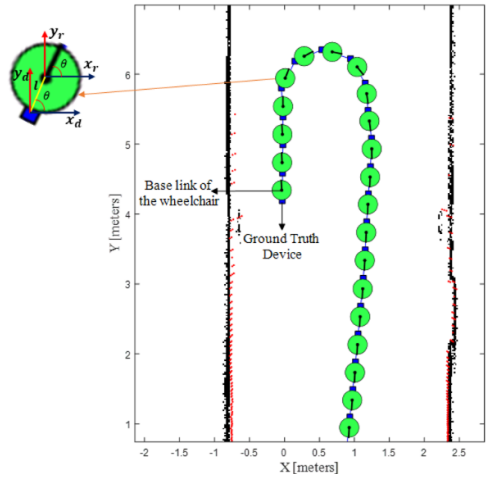

Figure 11

Trajectory of the mobile robot equipped with the developed device

This coordinate transformation is carried out using Eq. (1) and Eq. (2). Here, x_r and y_r denote the position of the mobile robot, while x_d and y_d refer to the position of the marker, all expressed in the global coordinate frame. In the same frame, θ

represents the robot's orientation angle, which corresponds to the yaw angle measured by the device's embedded IMU sensor:

$$x_r = x_d + l\cos(\theta) \tag{1}$$

$$y_r = y_d + l\sin(\theta) \tag{2}$$

As the developed device is rigidly mounted on the mobile robot, both share an identical orientation. Consequently, no additional rotational transformation is required when transferring the device's position data to the base link frame of the robot. Figure 12 presents a comparative analysis of the ground truth pose data obtained during the experimental phase and the two-dimensional pose estimates produced by the AMCL and Odometry algorithms. When the graph is examined, it is seen that although the estimation vector calculated with Odometry is very close to the ground truth data at the beginning, an error occurs over time and this error increases cumulatively. In the AMCL algorithm, however, it can be said that although instantaneous position errors may occur by using Lidar measurement data taken from the surroundings, these errors are eliminated or significantly reduced over time.

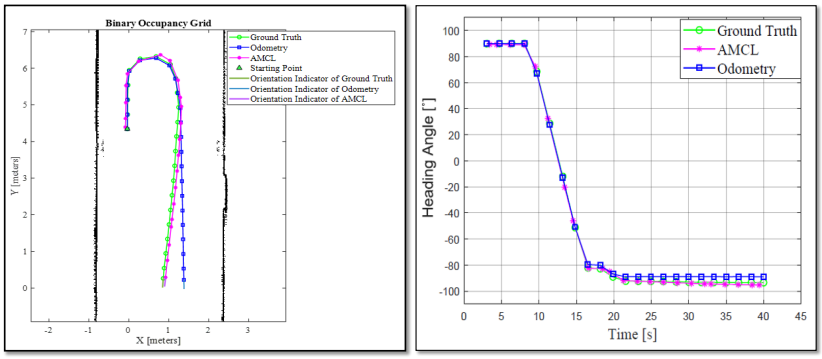

(a) (b)

Figure 12

To further evaluate the performance of the localization algorithms with respect to the ground truth data, 2D position and orientation error graphs were generated, as illustrated in Figure 13. As illustrated in the figure, the position estimation errors in the Odometry method exhibit a cumulative increase over time. In contrast, although the AMCL algorithm initially produces relatively large instantaneous errors, these errors tend to decrease progressively in the subsequent steps. The quantitative performance results of both algorithms are summarized in Table 1.

Table 1
The performance results of localization algorithms

Algorithms	Average 2D Positioning Error (m)	Standard Deviation (m)	Average Absolute Heading Error (°)
AMCL	0.1197	0.0631	1.7813
Odometry	0.1616	0.1716	2.6093

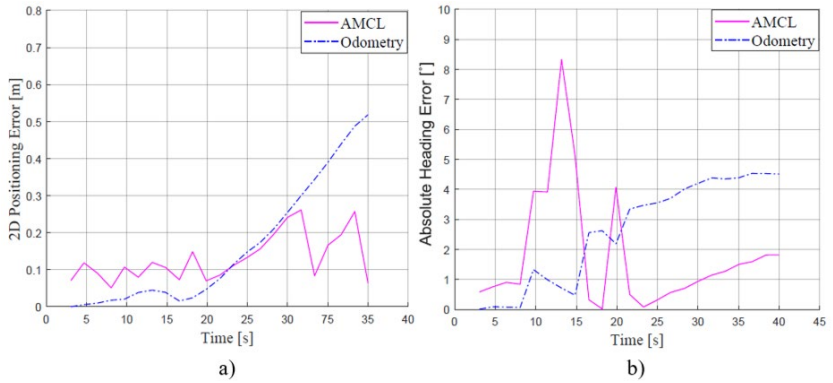

Figure 13
2D positioning error (a) and absolute heading error (b)

Conclusions

In this study, a simple and cost-effective device that can be easily mounted on various autonomous ground robots has been developed to facilitate the acquisition of ground truth pose information. Leveraging its ability to leave physical marks on the ground, the device enables extensive usage along the robot's entire trajectory. The fabrication of the developed device has been carried out with 3D printing technology using various thermoplastic materials.

The custom PCB card has been designed and fabricated to fulfill the tasks of integrating electronic components, motor control, and transmitting IMU sensor data with time of receipt to the main computer via wireless communication. Furthermore, a user interface has been developed to enable remote control of the device, offering two operational modes – automatic and manual – for regulating how the device leaves marks on the ground. The ROS platform has been used to capture the moment when the device left its mark on the ground and the orientation angle information at that moment, and transmit it to the main computer.

The performance of the developed device has been evaluated using AMCL and the Odometry-based localization method. For this purpose, the autonomous wheelchair platform designed within the scope of this study has been utilized as the ground robot model, while experimental validations have been conducted in the corridor of the Smart and Autonomous Systems Laboratory at the Faculty of Electrical and Electronics, Istanbul Technical University.

The device, mounted on the autonomous wheelchair, which has a speed of 0.25 m/s, has been operated in automatic mode with a period of 1.7 seconds and has left marks on the ground at specific intervals. The position of each mark has been measured manually to confirm the accuracy of the measurements taken automatically by the device.

The data obtained with the device has been compared with AMCL and Odometry data. As a result of this comparison, it is seen that the estimation vector calculated with Odometry is very close to the ground truth data at the beginning, but an error occurs over time, and this error increases cumulatively over time. In the AMCL algorithm, however, although instant position errors occur using Lidar measurement data taken from the surroundings, these errors decrease significantly in the next steps. According to the obtained results, the inferior performance of the position and orientation estimation based on Odometry compared to the AMCL approach is attributed to the drift effect.

Future research will aim to conduct a systematic performance comparison between conventional localization algorithms and novel approaches through the integration of the developed device into diverse ground robotic systems.

Acknowledgments

This work was supported by the Turkish Scientific and Technological Research Council (TUBITAK) under project no. 121E537.

References

[1] Kovič, K., Ojsteršek, R., and Palčič, I., 2023, Simultaneous Use of Digital Technologies and Industrial Robots in Manufacturing Firms, *Appl. Sci.*, 13 (10), p. 5890

[2] Aguiar, AS., dos Santos, FN., Cunha, JB., Sobreira, H. and Sousa, AJ., 2020, Localization and mapping for robots in agriculture and forestry: A survey, *Robotics*, 9(4), p. 97

[3] Ghobadpour, A., Monsalve, G., Cardenas, A., and Mousazadeh, H., 2022, Off-road electric vehicles and autonomous robots in agricultural sector: trends, challenges, and opportunities, *Vehicles*, 4(3), pp. 843-864

[4] Cañas, JM., Perdices, E., García-Pérez, L., and Fernández-Conde, J., 2020, A ROS-based open tool for intelligent robotics education, *Appl. Sci.*, 10(21), p. 7419

[5] Alverhed, E., Hellgren, S., Isaksson, H., Olsson, L., Palmqvist, H., and Flodén, J., 2024, Autonomous last-mile delivery robots: a literature review, *Eur. Transp. Res. Rev.*, 16(1), p. 4

[6] Mahajan, S., and Vidhyapathi CM., 2017, Design of a medical assistant robot, in *2017 2nd IEEE International Conference on Recent Trends in Electronics, Information & Communication Technology (RTEICT)*, pp. 877-881

[7] Altinpinar, OV., Contarli, EC., Kağizman, A., Uguzlar, U., Cansu, E., and Sezer, V., 2022, Comparison of Autonomous Robot's Mapping Performance Based on Number of Lidars And Number of Tours, in *2022 Innovations in Intelligent Systems and Applications Conference (ASYU)*, pp. 1-6

[8] KAĞIZMAN, A., and ALTUĞ, E., 2019, Otonom Araçlarda Navigasyon İçin Düşük Maliyetli, Taşınabilir ve [360]^ 0 Görüş Alanına Sahip Yeni Bir 3B LIDAR Sisteminin Geliştirilmesi, *Süleyman Demirel Üniversitesi Fen Bilim. Enstitüsü Derg.*, 23 (3), pp. 759-769

[9] Kaymaz, M., Ayzit, R., Akgün, O., Atik, K. C., Erdem, M., Yalcin, B., ... and Ure, NK., 2024, Trading-Off Safety with Agility Using Deep Pose Error Estimation and Reinforcement Learning for Perception-Driven UAV Motion Planning, *Journal of Intelligent & Robotic Systems*, *110* (2), 55

[10] Altınpınar, OV., and Sezer, V., 2023, A novel indoor localization algorithm based on a modified EKF using virtual dynamic point landmarks for 2D grid maps, *Rob. Auton. Syst.*, 170, pp. 104546

[11] Panigrahi, PK., and Bisoy, SK., 2022, Localization strategies for autonomous mobile robots: A review, *J. King Saud Univ. Inf. Sci.*, 34(8), pp. 6019-6039

[12] Belkin, I., Abramenko, A. and Yudin, D., 2021, Real-time lidar-based localization of mobile ground robot, *Procedia Comput. Sci.*, 186, pp. 440-448

[13] Altınpınar, OV., and Sezer, V., 2024, Real-Time Localization Application of MEKF-VDPL Algorithm on Autonomous Wheelchair in a Dynamic Environment, in 2024 15th National Conference on Electrical and Electronics Engineering (ELECO), pp. 1-5

[14] Sezer, V., Zengin, RS., Houshyari, H., and Yilmaz, MC., 2020, Conversion of a conventional wheelchair into an autonomous personal transportation testbed, *Serv. Robot*

[15] Yilmaz, A., and Temeltas, H., 2019, Self-adaptive Monte Carlo method for indoor localization of smart AGVs using LIDAR data, *Rob. Auton. Syst.*, 122, p. 103285

[16] Altınpınar, OV., Contarlı, EC., and Sezer, V., 2024, Real-Time Implementation of MEKF using VDPL Localization Algorithm by Utilizing MATLAB & ROS Communication, In *2024 Innovations in Intelligent Systems and Applications Conference (ASYU)*, pp. 1-6

[17] Richardson, JD., Hayes, WF., and Rossmeier, MB., 2016, Motion Capture Camera with Illuminated Status Ring. Google Patents, Feb. 11

[18] Yoshida, T., *et al.*, 2023, A Survey of Ground Truth Measurement Systems for Indoor Positioning, *J. Inf. Process.*, 31, pp. 15-20

[19] Sorokumov, S., Glazunov, S., and Chaika, K., Distributed Visual-Based Ground Truth System For Mobile Robotics

[20] Hu, H., Cao, Z., Yang, X., Xiong, H., and Lou, Y., 2021, Performance evaluation of optical motion capture sensors for assembly motion capturing, *IEEE Access*, 9, pp. 61444-61454

[21] Bostelman, R., Falco, J., and Hong, T., 2016, Performance measurements of motion capture systems used for AGV and robot arm evaluation

[22] Castillo, B., Riascos, C., Franco, J. M., Marulanda, J., and Thomson, P., 2025, Assessing spatiotemporal behavior of human gait: a comparative study between low-cost smartphone-based mocap and optitrack systems, *Experimental Techniques,* 49 (1), pp. 3-13

[23] Jakob, V., Küderle, A., Kluge, F., Klucken, J., Eskofier, B. M., Winkler, J., ... and Gassner, H., 2021, Validation of a sensor-based gait analysis system with a gold-standard motion capture system in patients with Parkinson's disease, *Sensors*, *21* (22), 7680

[24] Kirkpatrick, M., Sander, D., El Kalach, F., and Harik, R., 2023, Motion capture based calibration for industrial robots, *Manufacturing Letters*, *35*, pp. 926-932

[25] Sezer, V., and Kağızman, A., 2025, True location and orientation acquisition device for land robots, U.S. Patent Application No. 18/878,085, doi: https://doi.org/10.5281/zenodo.14781740

[26] Wasisto, I., Istiqomah, N., Trisnawan, IKN., and Jati, AN., 2019, Implementation of mobile sensor navigation system based on adaptive Monte Carlo localization, in *2019 International Conference on Computer, Control, Informatics and its Applications (IC3INA)*, pp. 187-192

[27] Xiaoyu, W. Caihong, LI., Li, S., Ning, Z., and Hao, FU., 2018, On adaptive monte carlo localization algorithm for the mobile robot based on ROS, in *2018 37th Chinese Control Conference (CCC)*, pp. 5207-5212

[28] Chung, MA., and Lin, CW., 2021, An improved localization of mobile robotic system based on AMCL algorithm, *IEEE Sensors Journal*, *22* (1), pp. 900-908

[29] Chen, B., Zhao, H., Zhu, R., and Hu, Y., 2022, Marked-LIEO: Visual marker-aided LiDAR/IMU/encoder integrated odometry, *Sensors*, *22* (13) 4749

[30] Kagizman, A., and Sezer, V., 2024, Design and fabrication of a new chest compression device with a specialized piston and bayonet lock mechanism, *Engineering Science and Technology, an International Journal*, *55,* 101724

[31] Amsters, R., and Slaets, P., 2020, Turtlebot 3 as a robotics education platform. In *Robotics in Education: Current Research and Innovations 10*, Springer International Publishing., pp. 170-181

[32] Jasim, S., and Sabr, H., 2016, Design and Implement of a Real Time Health Monitoring FHSSS Using NRF24L01 Transceiver, *13th international*

conference "standardization, protypes and quality: a means of balkan countries' collaboration", pp. 367-373

[33] Pokress, S., and Veiga, J., 2013, MIT App Inventor: Enabling personal mobile computing. In Workshop on Programming for Mobile and Touch

[34] Quigley, M., Conley, K., Gerkey, B., Faust, J., Foote, T., Leibs, J., ... and Ng, AY., 2009, ROS: an open-source Robot Operating System. In *ICRA workshop on open source software*, 3 (3.2) p. 5

[35] Somlyai, L., and Vámossy, Z., 2024, Improved RGB-D Camera-Based SLAM System for Mobil Robots. *Acta Polytechnica Hungarica* 21(8), pp. 107-24

[36] Zhang, L., Zapata, R., & Lepinay, P., 2012, Self-adaptive Monte Carlo localization for mobile robots using range finders, *Robotica*, 30 (2), pp. 229-244